Electronic Supplementary Information (ESI)

Linker Installation Transformations in a 2-D Rare Earth MOF: Increase of the Dimensionality and Turn on of the Temperature Sensing Capability

Laoura Komodiki[a], Nikos Panagiotou[a], Hélène Serier-Brault[b]*, Anastasios J. Tasiopoulos[a]*

[a]Department of Chemistry, University of Cyprus, 1678 Nicosia, Cyprus. E-mail: atasio@ucy.ac.cy

[b]Nantes Université CNRS Institut des Matériaux de Nantes Jean Rouxel, IMN Nantes F-44000, France. E-mail: helene.brault@cnrs-imn.fr

Table of Contents

Abbreviations

The abbreviations of the organic molecules discussed in ESI are the following: H_2BCPM = 4,4'-(hydroxymethylene)dibenzoic acid; H_2BDC = 1,4 benzenedicarboxylic acid); H_2ABDC = 2-aminobenzene-1,4-dicarboxylic acid; H_2FBDC = 2-fluorobenzene-1,4-dicarboxylic acid; H_2NDC = 1,4-naphthalenedicarboxylic acid; HFBA = 2-fluorobenzoic acid; TFA = trifluoroacetic acid; DMF = *N,N*-dimethylformamide; DMSO = dimethyl sulfoxide

Experimental Part

Materials

Reagent grade chemicals were obtained from commercial sources (Aldrich, Merck, Alfa Aesar, TCI, etc.) and used without further purification. All synthetic procedures were carried out in air. Other chemical reagents and solvents were of analytical grade and used without further purification.

Table S1: The Eu^{3+}/Tb^{3+} composition of the pristine MOF **UCY-17**($Eu_{0.05}Tb_{0.95}$) and the exchanged analogues **UCY-17**($Eu_{0.05}Tb_{0.95}$)/L (L = BDC^{2-}, $ABDC^{2-}$, $FBDC^{2-}$ and NDC^{2-}) determined by ICP-AES (Inductively Coupled Plasma – Atomic Emission Spectrometry).

Theoretical composition	ICP composition
UCY-17($Eu_{0.05}Tb_{0.95}$)	$Eu_{0.063}Tb_{0.937}$
UCY-17($Eu_{0.05}Tb_{0.95}$)/BDC	$Eu_{0.058}Tb_{0.942}$
UCY-17($Eu_{0.05}Tb_{0.95}$)/ABDC	$Eu_{0.059}Tb_{0.941}$
UCY-17($Eu_{0.05}Tb_{0.95}$)/FBDC	$Eu_{0.064}Tb_{0.936}$
UCY-17($Eu_{0.05}Tb_{0.95}$)/NDC	$Eu_{0.062}Tb_{0.938}$

Crystallographic Data

Table S2: Selected Crystal Data for compounds **UCY-17**(RE).

Compound	**UCY-17**(Y)	**UCY-17**(Gd)	**UCY-17**(Tb)	**UCY-17**(Dy)	**UCY-17**(Ho)	**UCY-17**(Er)
Empirical formula	$C_{30}H_{18}NO_{19}Y_3$	$C_{30}H_{18}NO_{19}Gd_3$	$C_{30}H_{18}NO_{19}Tb_3$	$C_{30}H_{18}NO_{19}Dy_3$	$C_{30}H_{18}NO_{19}Ho_3$	$C_{30}H_{18}NO_{19}Er_3$
Formula weight	963.18	1168.20	1173.25	1183.96	1191.24	1198.23
Temperature / K	293(2)	145(2)	104(4)	102(1)	102(2)	104(2)
Wavelength / Å	1.54184	1.54184	1.54184	1.54184	1.54184	1.54184
Crystal system	Monoclinic	Monoclinic	Monoclinic	Monoclinic	Monoclinic	Monoclinic
Space group	*C 2/m*	*C 2/m*	*C 2/m*	*C 2/m*	*C 2/m*	*C 2/m*
a / Å	29.6715(3)	30.1356(7)	29.8060(8)	29.9207(7)	29.5465(5)	29.7195(6)
b / Å	18.3115(2)	18.2215(7)	18.4881(7)	18.2577(5)	18.6021(4)	18.1534(5)
c / Å	14.5989(1)	14.6429(4)	14.6432(4)	14.6257(4)	14.5637(3)	14.5912(3)
$\alpha = \gamma$ / °	90	90	90	90	90	90
β / °	101.951 (1)	100.531(2)	100.960(3)	100.432(2)	102.304(2)	101.482(2)
Volume / Å^3	7760.1(2)	7905.2(4)	7922.0(4)	7857.7(4)	7820.7(3)	7714.6(3)
Z	4	4	4	4	4	4
$d_{calc.}$/ g/cm^3	0.824	0.982	0.984	1.001	1.012	1.032
Absorption coefficient / mm^{-1}	3.276	16.377	13.269	15.362	5.767	6.158
F(000)	1896	2196	2113	2119	2232	2244
Reflections collected	42780	46765	27095	27408	25371	24940
Independent reflections	7147	7281	7291	7238	7197	7115
Completeness to θ = 66.99°	99.7% [R_{int} = 0.0399]	100% [R_{int} = 0.0755]	99.9% [R_{int} = 0.0566]	99.9% [R_{int} = 0.0474]	99.8% [R_{int} = 0.0344]	99.8% [R_{int} = 0.0225]
Data / restraints / parameters	7147/17/248	7281/23/247	7291/22/247	7238/22/247	7197/22/247	7115/4/247
Goodness-of-fit	1.086	0.958	0.994	0.984	1.093	1.116
Final R indices [I > 2σ(I)]	R_1 = 0.0609, wR_2 = 0.1938	R_1 = 0.0668, wR_2 = 0.1937	R_1 = 0.0597, wR_2 = 0.1729	R_1 = 0.0519, wR2 = 0.1508	R_1 =0.0511, wR_2 =0.1626	R_1 = 0.0436, wR_2 = 0.1412
R indices [all data]	R_1 = 0.0640, wR_2 = 0.1988	R_1 = 0.0836, wR_2 = 0.2059	R_1 = 0.0653, wR_2 = 0.1809	R_1 = 0.0593, wR_2 = 0.1594	R_1 =0.0559, wR_2= 0.1680	R_1 = 0.0463, wR_2 = 0.1437

Table S3: Selected Crystal Data for compounds **UCY-17**(Tb)/L.

Compound	**UCY-17**(Tb)/BDC	**UCY-17**(Tb)/ABDC	**UCY-17**(Tb)/FBDC	**UCY-17**(Tb)/NDC
Empirical formula	$C_{34}H_{20}O_{18}Tb_3$	$C_{68}H_{41}NO_{36}Tb_6$	$C_{68}H_{39}FO_{36}Tb_6$	$C_{36}H_{20}O_{18}Tb_3$
Formula weight	1193.26	2401.54	2404.51	1217.28
Temperature / K	100(2)	100(2)	100(2)	100(1)
Wavelength / Å	1.54184	1.54184	1.54184	1.54184
Crystal system	Monoclinic	Monoclinic	Monoclinic	Monoclinic
Space group	*C* 2/*m*	*C* 2/*m*	*C* 2/*m*	*C* 2/*m*
a / Å	29.812(2)	29.609(2)	29.7002(6)	18.795(2)
b / Å	18.891(3)	18.616(1)	18.5497(6)	29.712(2)
c / Å	14.834(2)	14.9895(5)	14.9529(3)	15.479(2)
$\alpha = \gamma$ / °	90	90	90	90
β / °	100.85(1)	99.990(4)	100.273(2)	102.31(1)
Volume / Å^3	8205 (2)	8137.0(6)	8106.0(4)	8445(2)
Z	4	2	2	4
$d_{calc.}$/ g/cm^3	0.966	0.980	0.985	0.957
Absorption coefficient / mm^{-1}	12.804	12.915	12.973	12.448
F(000)	2252	2268	2268	2300
Reflections collected	24220	17541	27258	16388
Independent reflections	7508	7448	7466	7626
Completeness to θ = 66.99°	99.3% [R_{int} =0.1156]	99.5% [R_{int}=0.0508]	99.9% [R_{int}= 0.0552]	99.2% [R_{int}= 0.0813]
Data / restraints / parameters	7508/298/232	7448/132/251	7466/45/254	7626/279/290
Goodness-of-fit	0.982	0.954	1.048	1.070
Final R indices [I > 2σ(I)]	R_1 = 0.1038, wR_2 = 0.2865	R_1 = 0.0903, wR_2 = 0.2392	R_1 = 0.0893, wR_2 = 0.2429	R_1 = 0.1170, wR_2 = 0.3044
R indices [all data]	R_1 = 0.1302, wR_2 = 0.3198	R_1 = 0.1094, wR_2 = 0.2502	R_1 = 0.0978, wR_2 = 0.2544	R_1 = 0.1356, wR_2 = 0.3283

Physical Measurements/Characterization of UCY-17(RE) (RE: Y, Gd, Tb, Dy, Ho, Er)

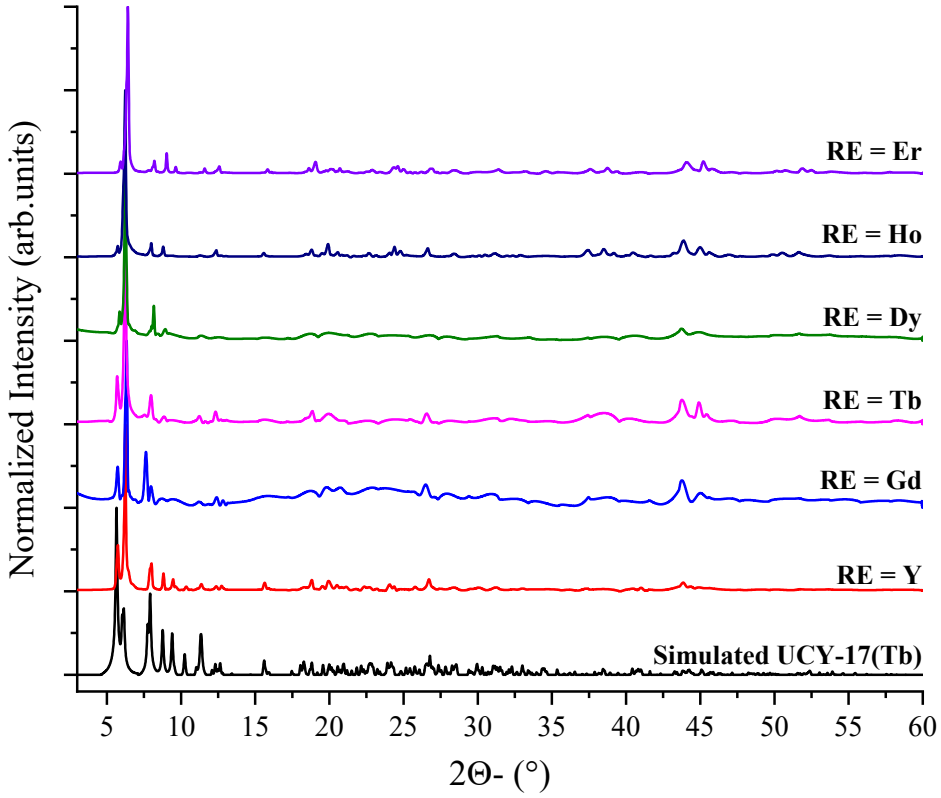

Figure S1: Powder X-ray diffraction patterns of the as synthesized compounds **UCY-17**(RE) along with the simulated pattern of **UCY-17**(Tb) from the single crystal data.

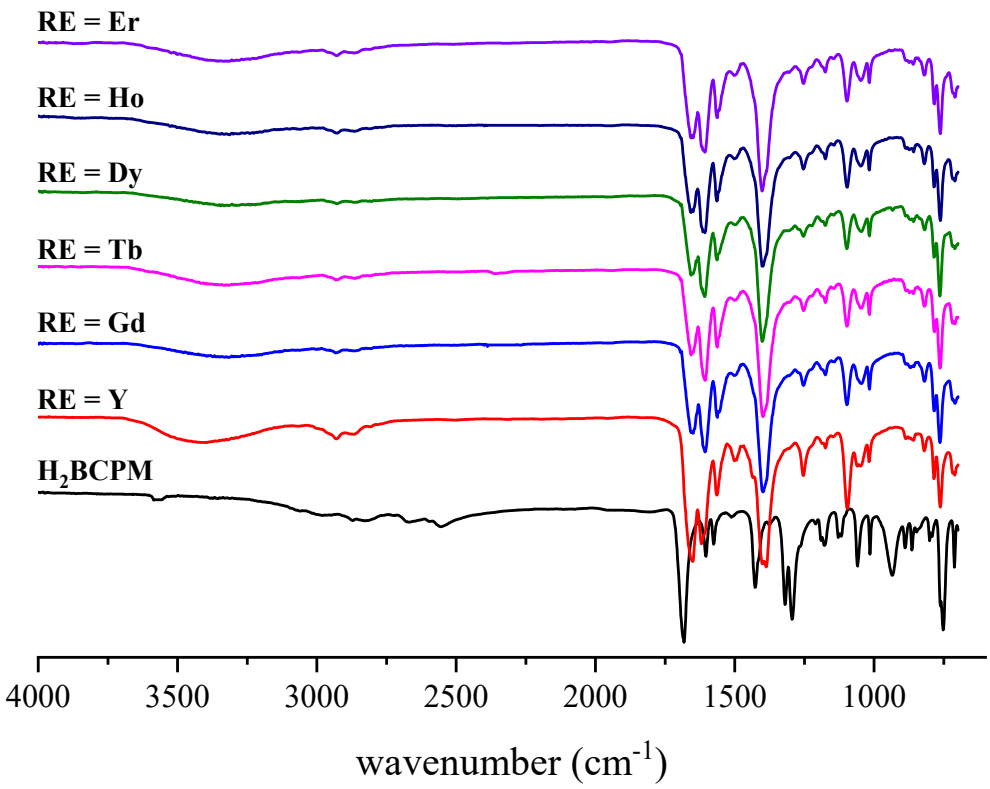

Figure S2: IR spectra of H_2BCPM ligand and the as synthesized compounds **UCY-17**(RE).

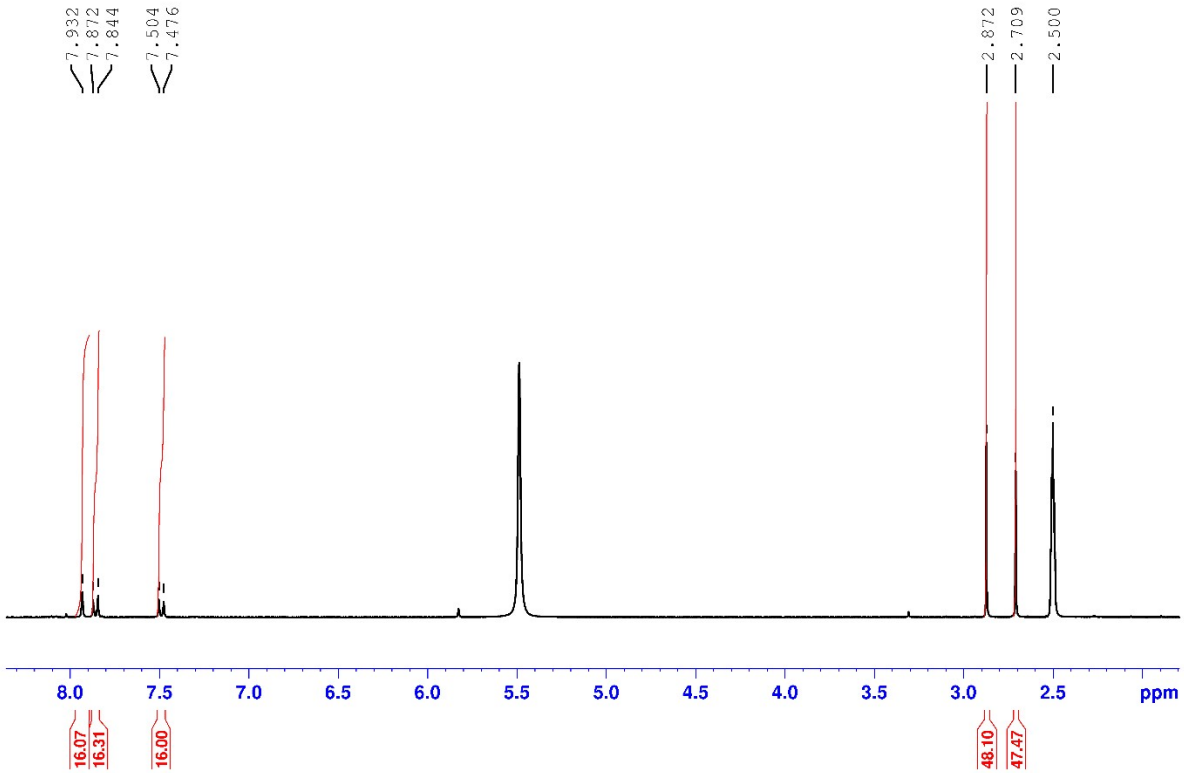

Figure S3: ^{1}H-NMR spectrum of as synthesized **UCY-17**(Y) digested in d_6-DMSO. These data indicate the presence of the organic ligand $BCPM^{2-}$ as well as DMF molecules in **UCY-17**(Y). ^{1}H NMR (DMSO): δ 2.500 (t, residual solvent peaks), δ 2.709 (s, 3H, C**H**$_3$, DMF), δ 2.872 (s, 3H, C**H**$_3$, DMF), δ 7.932 (s, H, C**H**O, DMF), δ 7.476-7.504 (d, 4H, Ar-**H**, $BCPM^{2-}$), δ 7.844 – 7.872 (d, 4H, Ar-**H**, $BCPM^{2-}$).

Determination of the amount of F^- anions per $(Gd^{3+})_6$ SBU in bulk UCY-17(Gd) microcrystalline powder: In order to quantify the amount of F^- anions per $(Re^{3+})_6$ SBU ^{19}Fq-NMR measurements were performed. For this purpose, a trifluoroacetic acid (TFA) solution in D_2O was used as an external standard. Prior the ^{19}Fq-NMR experiment, the concentration of the trifluoroacetic acid (TFA) solution was determined using NaF solutions with known concentration. Afterwards microcrystalline powder of **UCY-17**(Gd) (~ 10 – 15mg in each experiment) was digested in a 0.5M KOH solution in D_2O and then 500 μL of the resulting solution was transferred to the NMR tube along with the microprobe tube containing the external standard (the known concentration trifluoroacetic acid (TFA) solution). The experiment was repeated three times.[1,2]

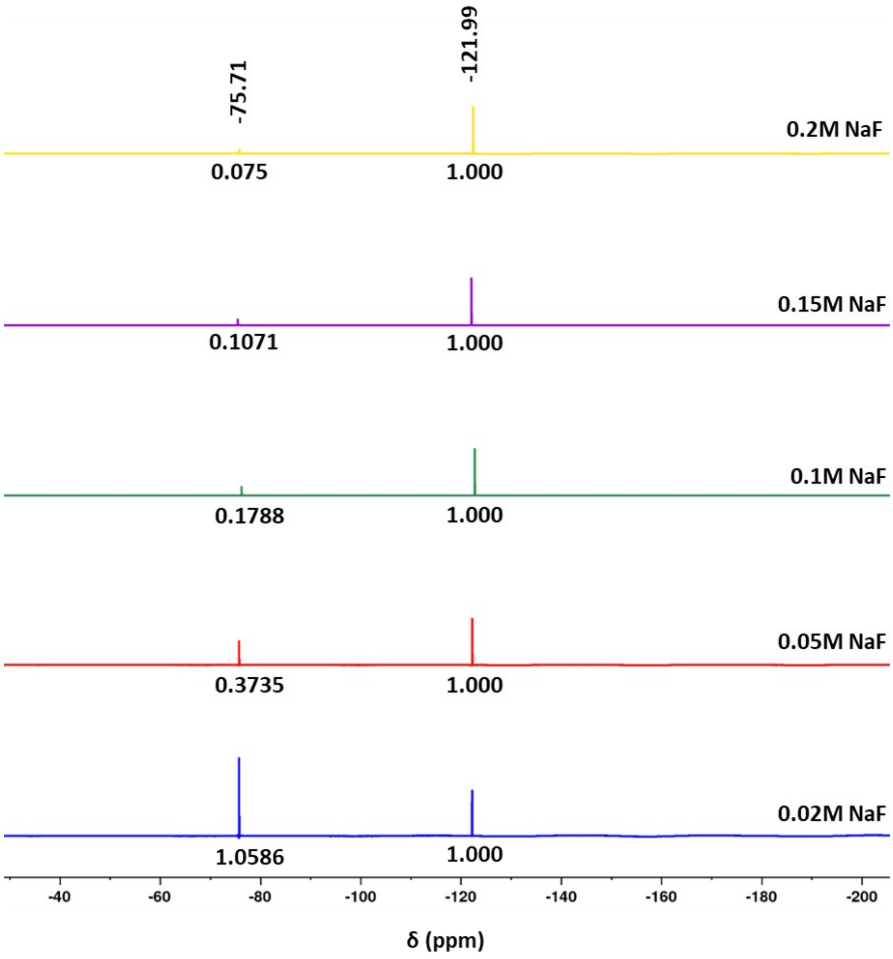

Figure S4: ^{19}Fq-NMR calibration spectra of the TFA solution external standard using NaF solutions of known concertation. TFA concentration was found equal to 5.9 ± 0.8mM. ^{19}F NMR (D_2O): δ -75.71 (TFA), δ -121.99 (F^-).

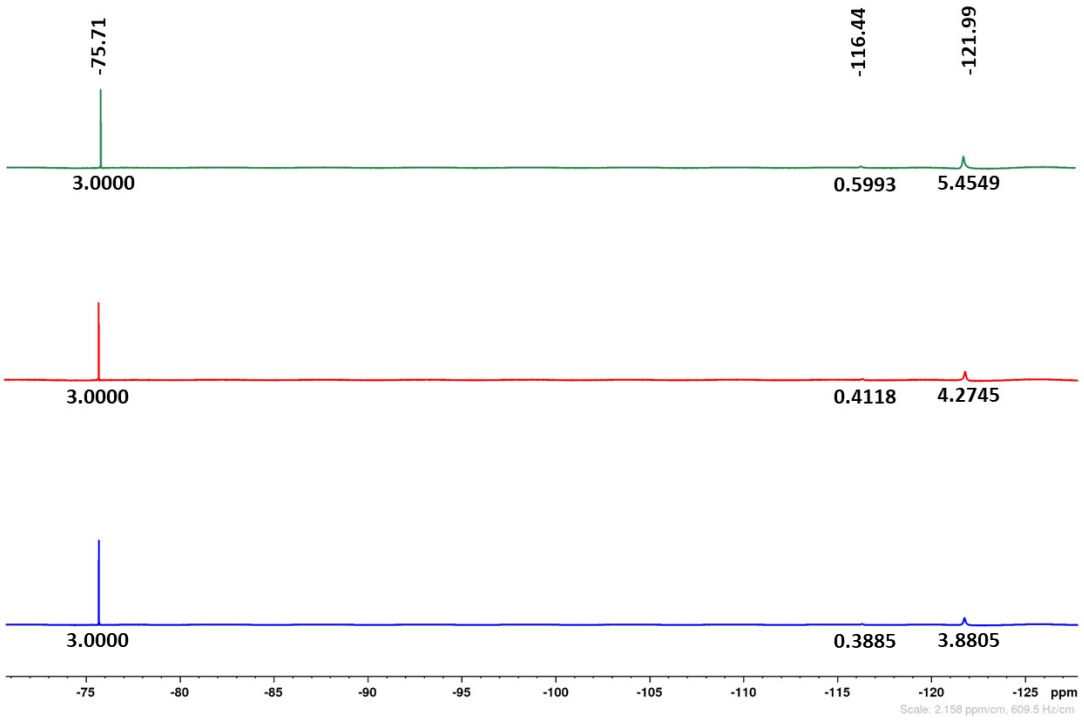

Figure S5: ^{19}Fq-NMR spectra of as synthesized **UCY-17**(Gd) digested in 0.5M KOH in D_2O along with the TFA solution (external standard). These studies indicated that **UCY-17**(Gd) contains ~ 1.6 ± 0.12 F^- anions / $(Gd^{3+})_6$ SBU. ^{19}F NMR (D_2O): δ -75.71 (TFA), δ -116.44 (FBA^-), δ -121.99 (F^-).

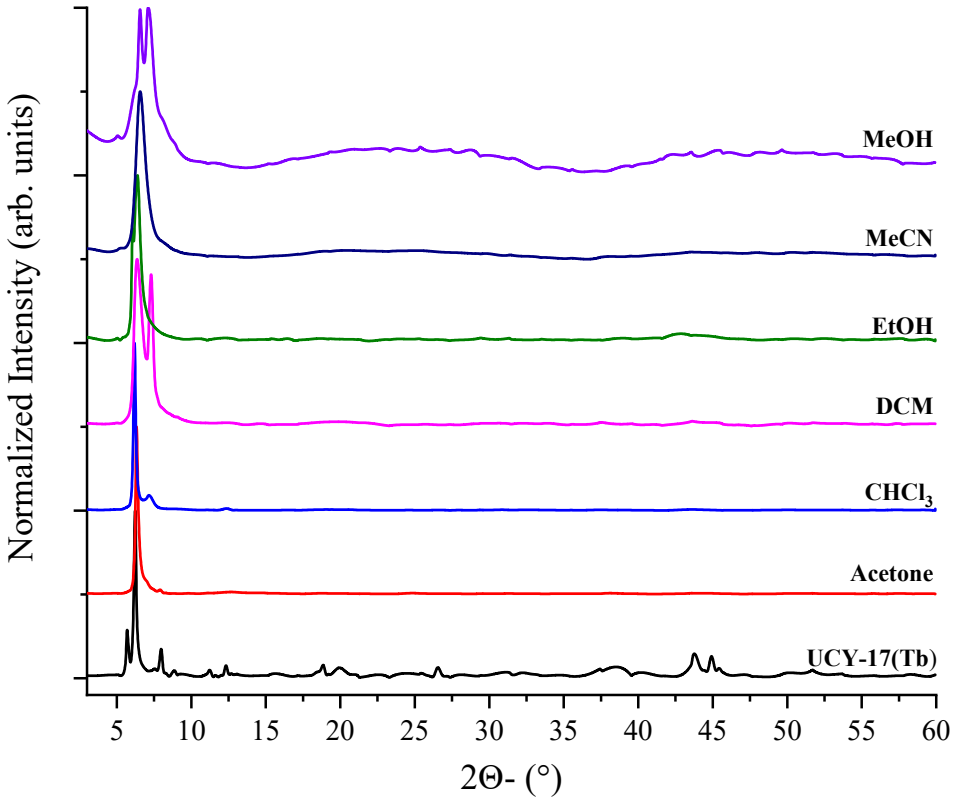

Figure S6: Powder X-ray diffraction patterns of as synthesized **UCY-17**(Tb) treated in various organic solvents for 10 days.

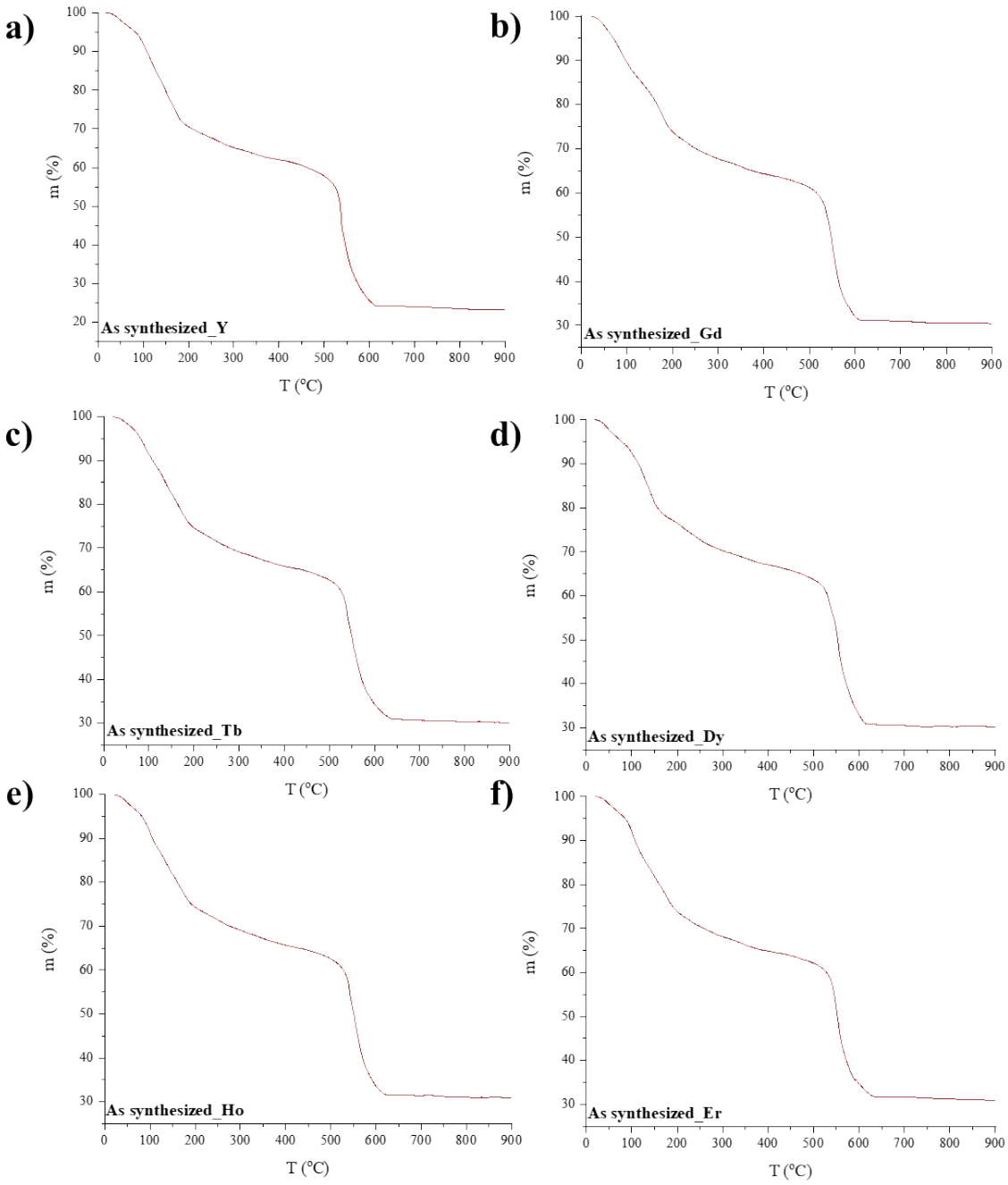

Figure S7: TGA graphs of the as synthesized compounds **UCY-17**(RE) (a) RE = Y, (b) RE = Gd, (c) RE = Tb, (d) RE = Dy, (e) RE = Ho, (f) RE = Er). TG analysis reveals that the thermal decomposition of compounds **UCY-17**(RE) proceeds via a two-step process. The first step (until ~400-450^{o}C) is attributed to the removal of the terminal water molecules and lattice DMF molecules. The second mass loss which is completed at ~620-640 ^{o}C is attributed to the decomposition of the ligand $BCPM^{2-}$. Lastly the residual mass at 900^{o}C corresponds to the rare earth oxide of the corresponding RE^{III} ion. Details on calculated values for solvent removal and ligand decomposition along with the experimental values obtained from TG analysis are shown in Table S4.

Table S4: Calculated values for solvent removal and ligand combustion along with the experimental values obtained from TG analysis for the as synthesized compounds **UCY-17**(RE).

Compound	Lattice Solvent Removal			Ligand Combustion		Residual Oxide		
	Temperature (°C)	Experimental (Calculated) (%)	xDMF	Temperature (°C)	Experimental (Calculated) (%)	Temperature (°C)	Experimental (Calculated) (%)	Formula
UCY-17(Y)	r.t. - 450	40 (40)	16	450 – 620	37 (38)	900	23 (22)	Y_2O_3
UCY-17(Gd)	r.t. - 450	37 (37)	17	450 – 620	32 (33)	900	31 (30)	Gd_2O_3
UCY-17(Tb)	r.t. - 450	36 (35)	16	450 - 640	34 (33)	900	30 (32)	Tb_4O_7
UCY-17(Dy)	r.t. – 450	34 (34)	15	450 - 620	35 (34)	900	31 (32)	Dy_2O_3
UCY-17(Ho)	r.t. - 450	36 (36)	17	450 - 620	33 (33)	900	31 (31)	Ho_2O_3
UCY-17(Er)	r.t. - 450	36 (36)	17	450 - 630	32 (33)	900	32 (31)	Er_2O_3

Physical Measurements/Characterization of UCY-17($Eu_{0.05}Tb_{0.95}$) and UCY-17(RE)/L; RE= Gd, Tb, $Eu_{0.05}Tb_{0.95}$, L=BDC^{2-}, $ABDC^{2-}$, $FBDC^{2-}$, NDC^{2-}

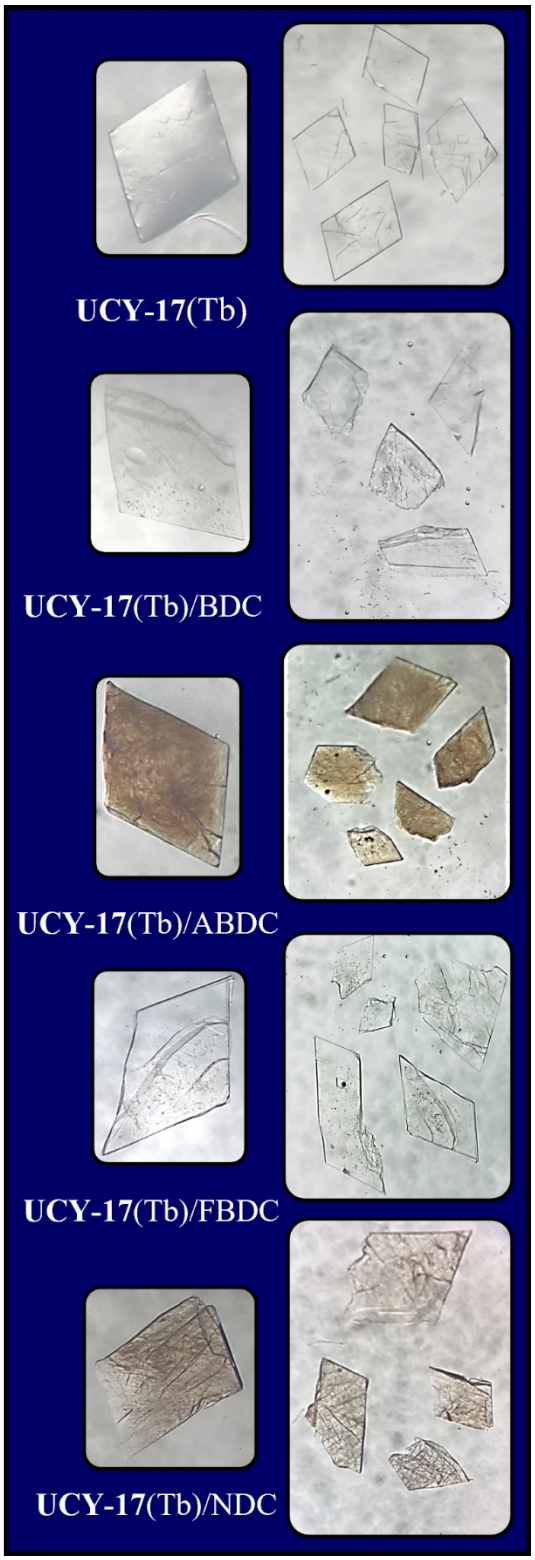

Figure S8: Stereoscope images of the crystals of **UCY-17**(Tb), **UCY-17**(Tb)/L; L= BDC^{2-}, $ABDC^{2-}$, $FBDC^{2-}$, NDC^{2-}.

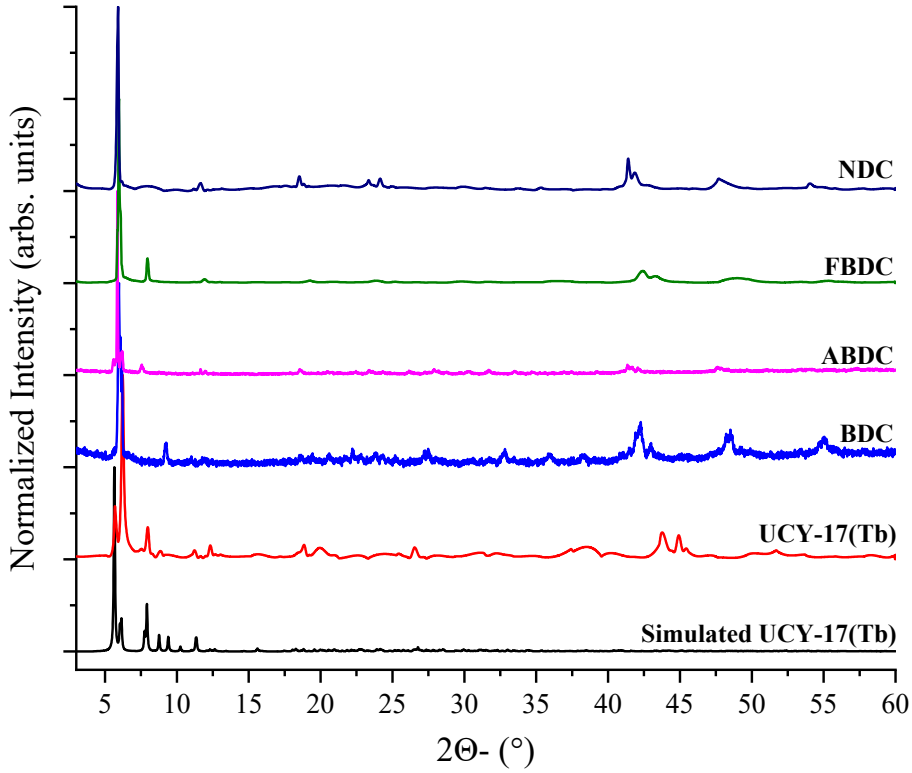

Figure S9: Powder X-ray diffraction patterns of **UCY-17**(Tb) and the exchanged analogues **UCY-17**(Tb)/L (L = BDC^{2-}, $ABDC^{2-}$, $FBDC^{2-}$ and NDC^{2-}) along with the simulated pattern of **UCY-17**(Tb) from the single crystal data.

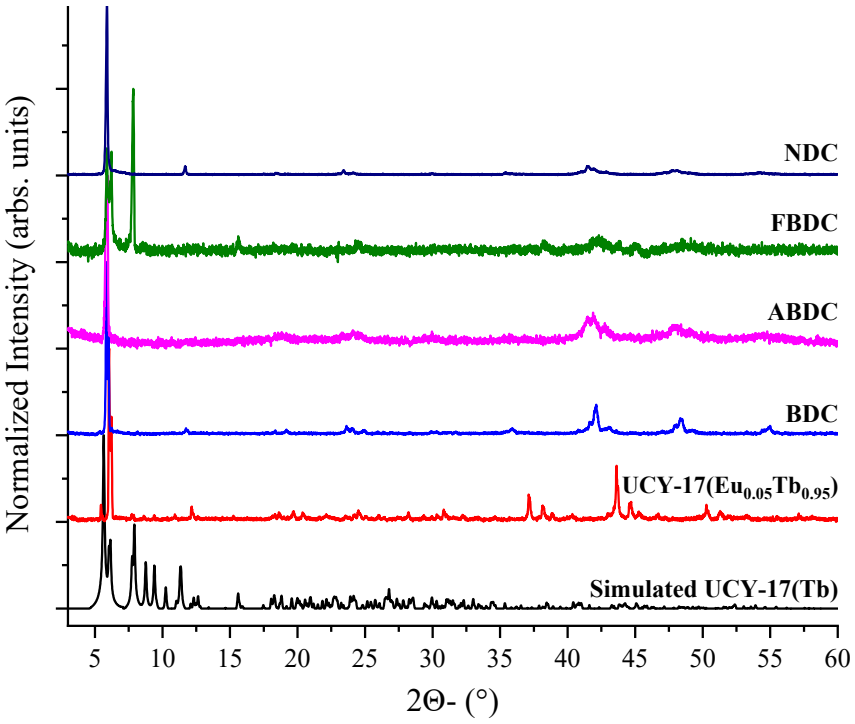

Figure S10: Powder X-ray diffraction patterns of the pristine MOF **UCY-17**($Eu_{0.05}Tb_{0.95}$) and the exchanged analogues **UCY-17**($Eu_{0.05}Tb_{0.95}$)/L (L = BDC^{2-}, $ABDC^{2-}$, $FBDC^{2-}$ and NDC^{2-}) along with the simulated pattern of **UCY-17**(Tb) from the single crystal data.

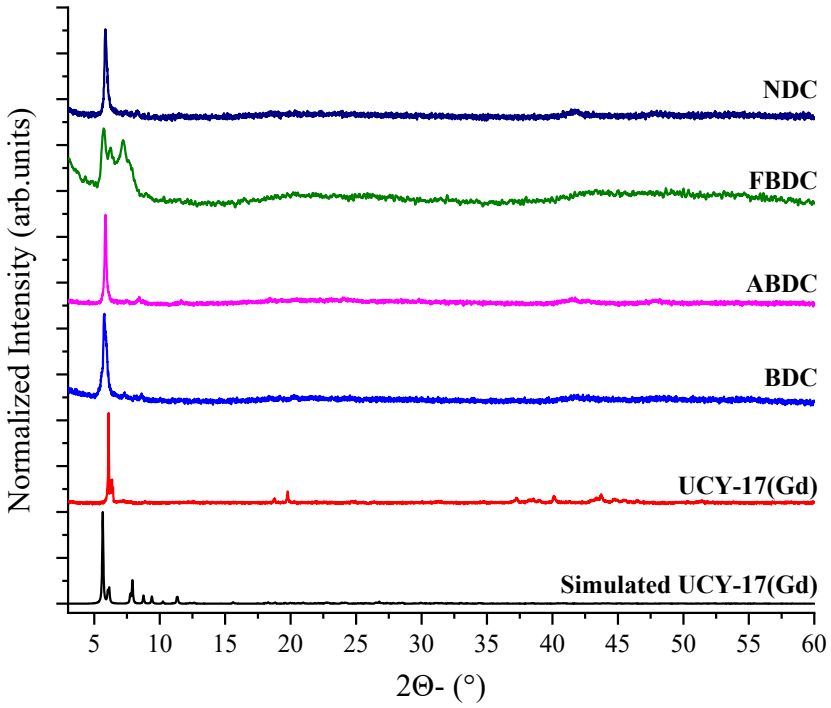

Figure S11: Powder X-ray diffraction patterns of the exchanged analogues **UCY-17**(Gd)/L (L = BDC^{2-}, $ABDC^{2-}$, $FBDC^{2-}$ and NDC^{2-}) along with the experimental and simulated patterns of **UCY-17**(Gd) from the single crystal data.

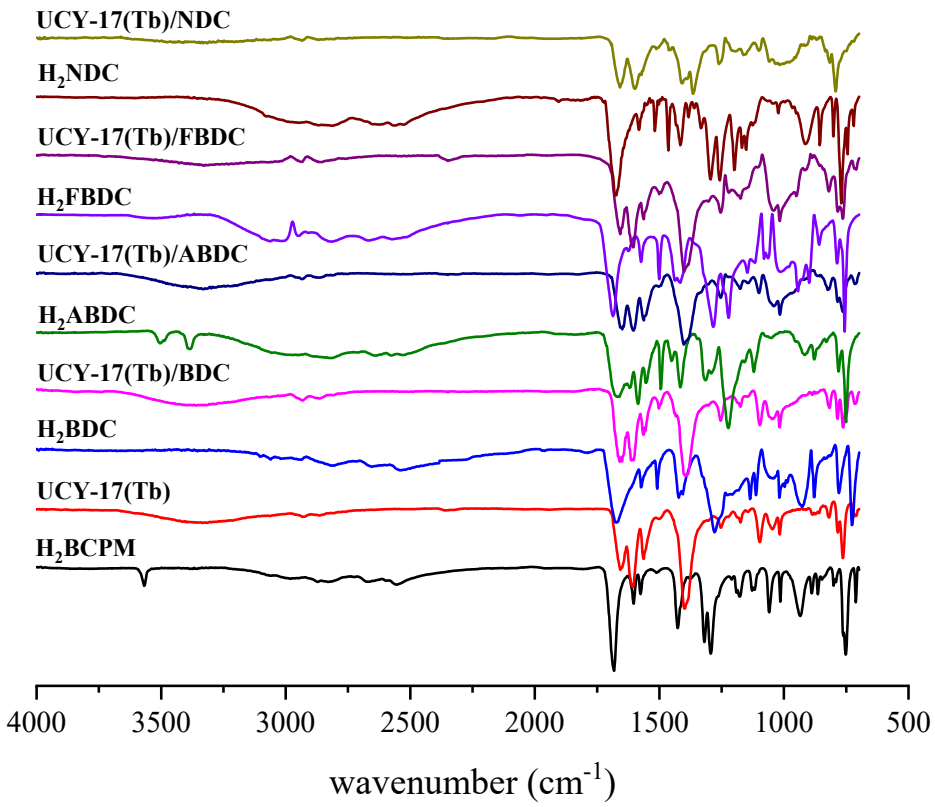

Figure S12: IR spectra of H_2BCPM, H_2BDC, H_2ABDC, H_2FBDC, H_2NDC ligands, the pristine MOF **UCY-17**(Tb) and the exchanged analogues **UCY-17**(Tb)/L (L = BDC^{2-}, $ABDC^{2-}$, $FBDC^{2-}$ and NDC^{2-}).

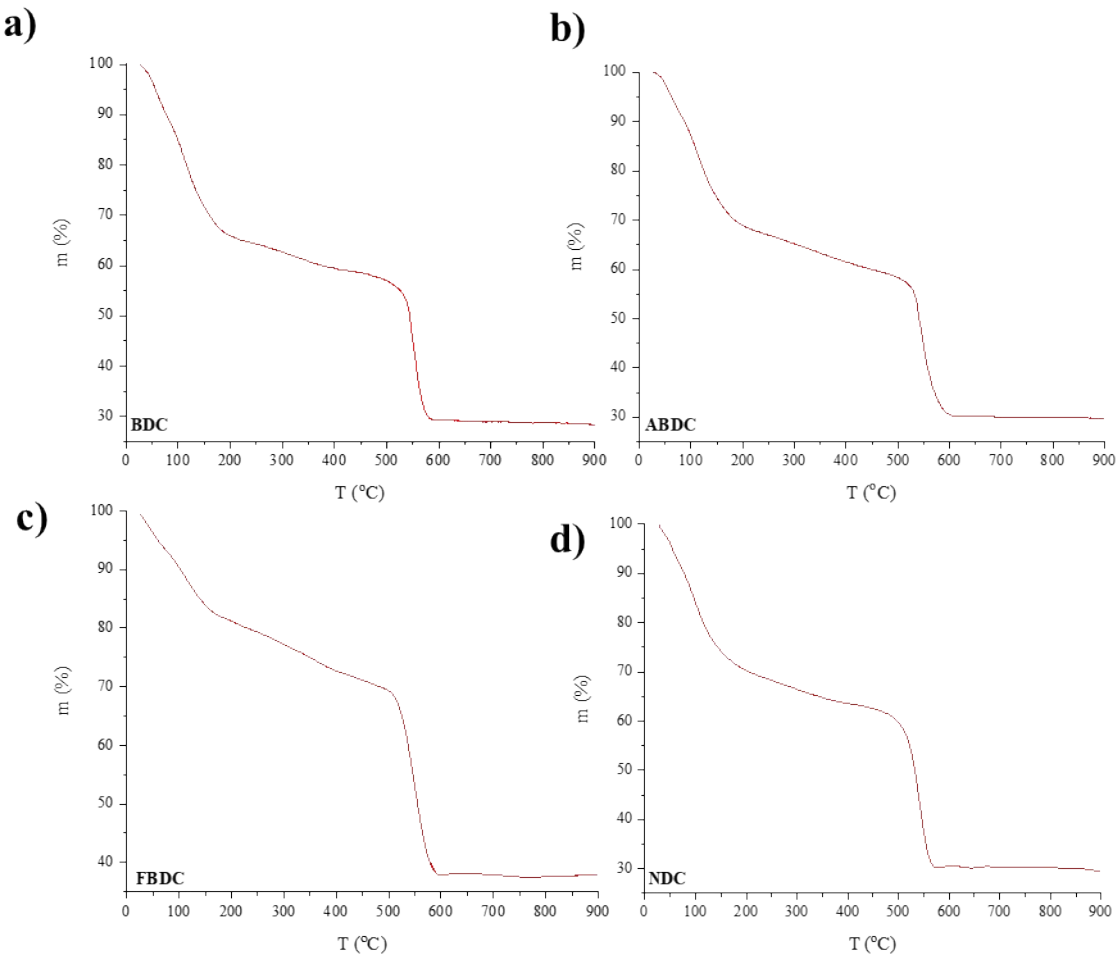

Figure S13: TGA graphs of the exchanged analogues **UCY-17(**Tb)/L (L = BDC^{2-}, $ABDC^{2-}$, $FBDC^{2-}$ and NDC^{2-}). TG analysis reveals that the thermal decomposition of compounds **UCY-17(**Tb)/L proceeds via a two-step process. The first step (until ~400-450°C) is attributed to the removal of the terminal water molecules and lattice DMF molecules. The second mass loss which is completed at ~600°C for **UCY-17(**Tb)/L is attributed to the decomposition of the ligands $BCPM^{2-}$ and L^{2-}. Lastly the residual mass at 900°C corresponds to Tb_4O_7. Details on calculated values for solvent removal and ligand decomposition along with the experimental values obtained from TG analysis are shown in Table S5.

Table S5: Calculated values for solvent removal and ligand combustion along with the experimental values obtained from TG analysis for the exchanged analogues **UCY-17**(Tb)/L (L = BDC^{2-}, $ABDC^{2-}$, $FBDC^{2-}$ and NDC^{2-})

Compound	Lattice Solvent Removal			Ligand Combustion		Residual Oxide		
	Temperature (°C)	Experimental (Calculated) (%)	xDMF	Temperature (°C)	Experimental (Calculated) (%)	Temperature (°C)	Experimental (Calculated) (%)	Formula
UCY-17(Tb)/BDC	r.t. - 450	41 (42)	22	450 - 600	30 (30)	900	29 (28)	Tb_4O_7
UCY-17(Tb)/ABDC	r.t. - 450	39 (39)	20	450 - 600	31 (30)	900	30 (29)	Tb_4O_7
UCY-17(Tb)/FBDC	r.t. – 400	27 (27)	11	400 - 600	36 (38)	900	37 (35)	Tb_4O_7
UCY-17(Tb)-NDC	r.t. – 450	37 (38)	19	450 - 600	33 (33)	900	30 (29)	Tb_4O_7

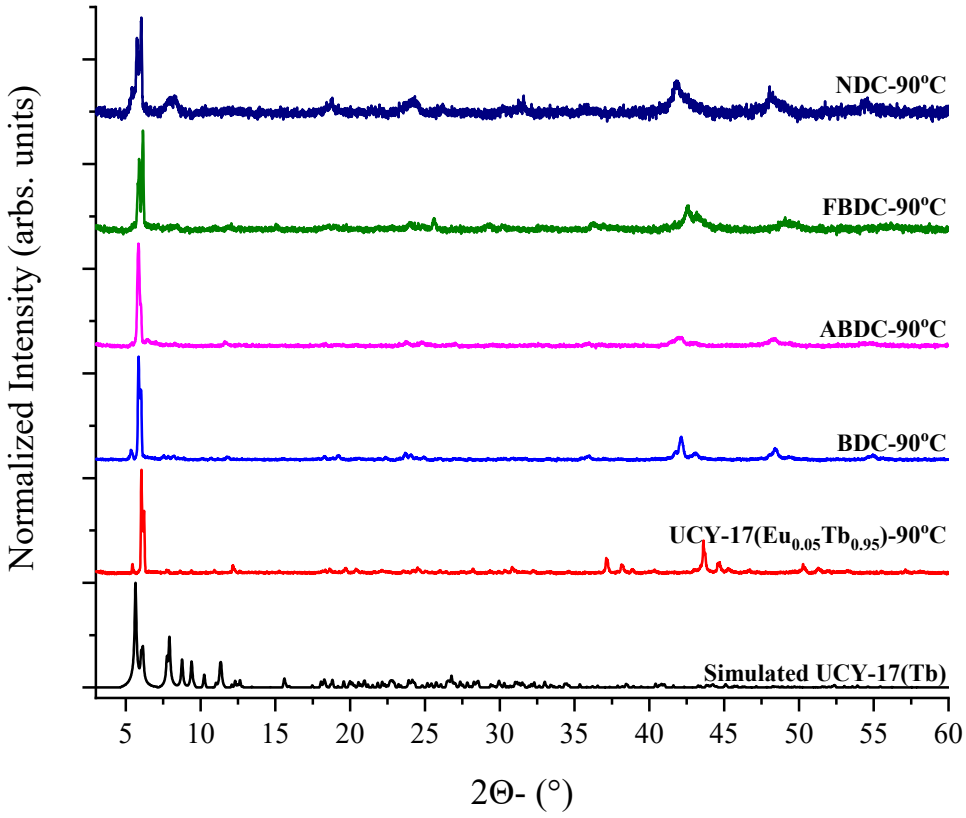

Figure S14: Powder X-ray diffraction patterns of the exchanged analogues **UCY-17**($Eu_{0.05}Tb_{0.95}$)/L (L = BDC^{2-}, $ABDC^{2-}$, $FBDC^{2-}$ and NDC^{2-}) along with the simulated pattern of **UCY-17**(Tb) from the single crystal data, after heating at 90°C (following the process described in the experimental part in the main manuscript).

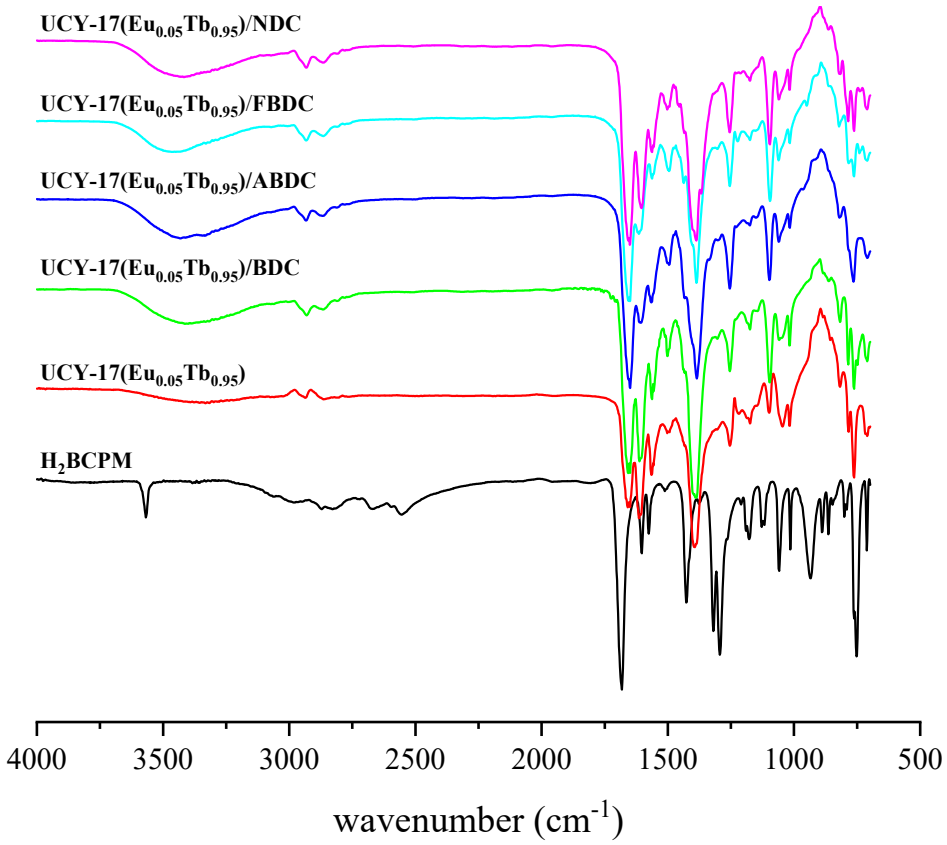

Figure S15: IR spectra of the pristine MOF **UCY-17**($Eu_{0.05}Tb_{0.95}$) and the exchanged analogues **UCY-17**($Eu_{0.05}Tb_{0.95}$)/L (L = BDC^{2-}, $ABDC^{2-}$, $FBDC^{2-}$ and NDC^{2-}).

a)

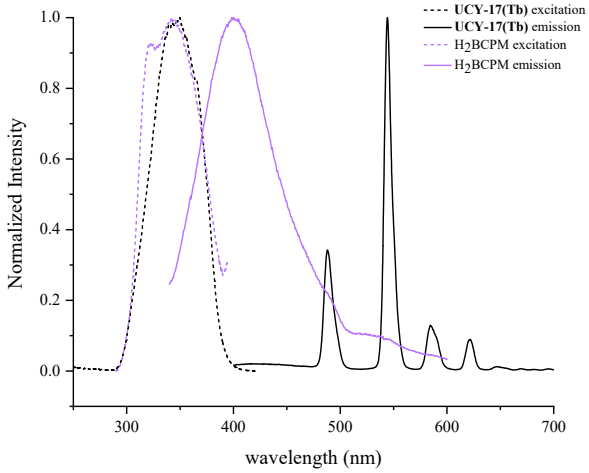

b)

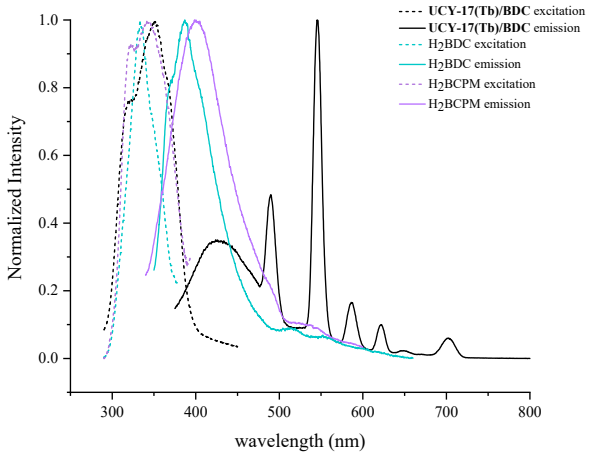

c)

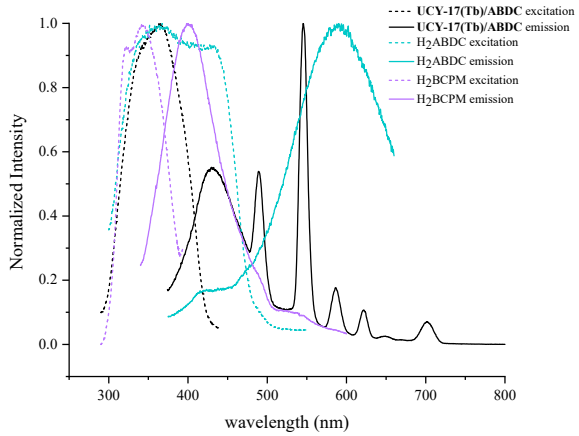

d)

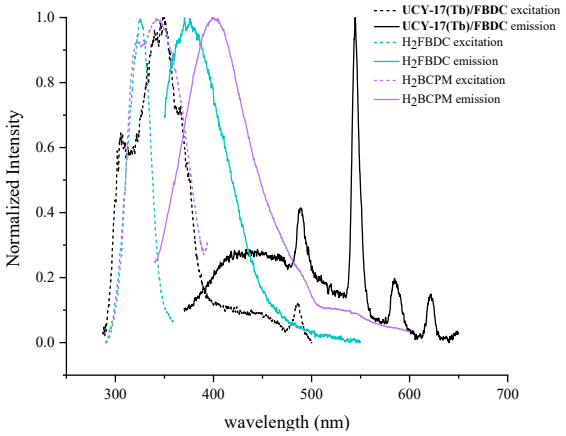

e)

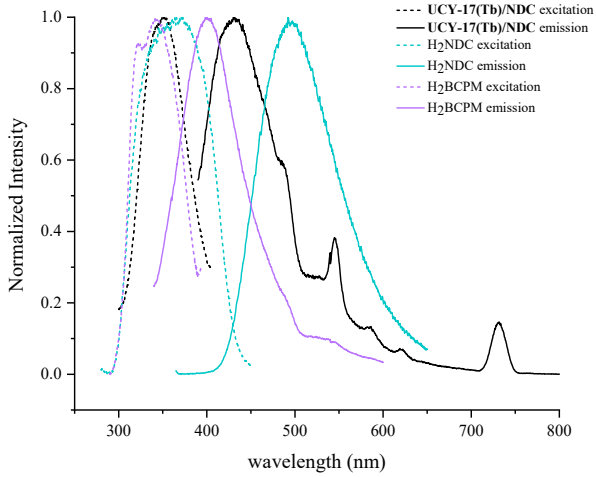

Figure S16: Solid-state emission and excitation spectra of a) **UCY-17**(Tb) ($\lambda_{exc.}$=345 nm and $\lambda_{em.}$=545 nm) and the organic ligand H_2BCPM ($\lambda_{exc.}$=345 nm and $\lambda_{em.}$=400 nm) b) **UCY-17**(Tb)/BDC ($\lambda_{exc.}$=350 nm and $\lambda_{em.}$=545 nm) and the organic ligands H_2BDC ($\lambda_{exc.}$=335 nm and $\lambda_{em.}$=387 nm) and H_2BCPM, c) **UCY-17**(Tb)/ABDC ($\lambda_{exc.}$=365 nm and $\lambda_{em.}$=545 nm) and the organic ligands H_2ABDC ($\lambda_{exc.}$=365 nm and $\lambda_{em.}$=588 nm) and H_2BCPM, d) **UCY-17**(Tb)/FBDC ($\lambda_{exc.}$=350 nm and $\lambda_{em.}$=545 nm) and the organic ligands H_2FBDC ($\lambda_{exc.}$=325 nm and $\lambda_{em.}$=375 nm) and H_2BCPM at room temperature, e) **UCY-17**(Tb)/NDC ($\lambda_{exc.}$=350 nm and $\lambda_{em.}$=545 nm) and the organic ligands H_2NDC ($\lambda_{exc.}$=365 nm and $\lambda_{em.}$=495 nm) and H_2BCPM.

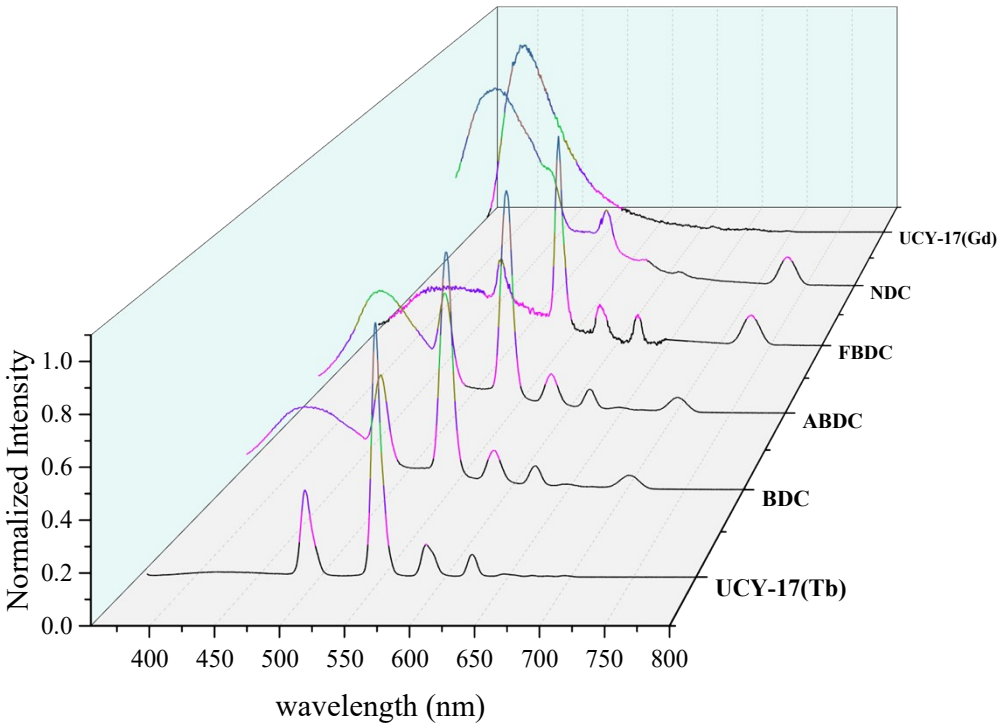

Figure S17: Solid-state emission spectra of compounds **UCY-17**(Tb), **UCY-17**(Tb)/L (L= BDC^{2-}, $ABDC^{2-}$, $FBDC^{2-}$, NDC^{2-}) and **UCY-17**(Gd) with λ_{exc}~ 350 nm.

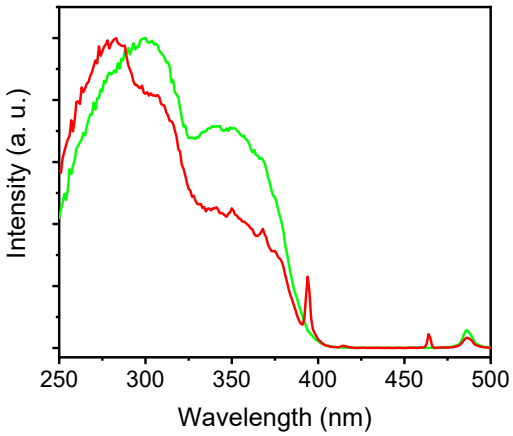

Figure S18: Room temperature excitation spectra of the pristine **UCY-17**($Eu_{0.05}Tb_{0.95}$) MOF monitoring the transitions $^5D_0 \nleftarrow {}^7F_2$ of Eu^{3+} (red solid line, λ_{em} = 614 nm) and $^5D_4 \nleftarrow {}^7F_5$ of Tb^{3+} (green solid line, λ_{em} = 543 nm) ions.

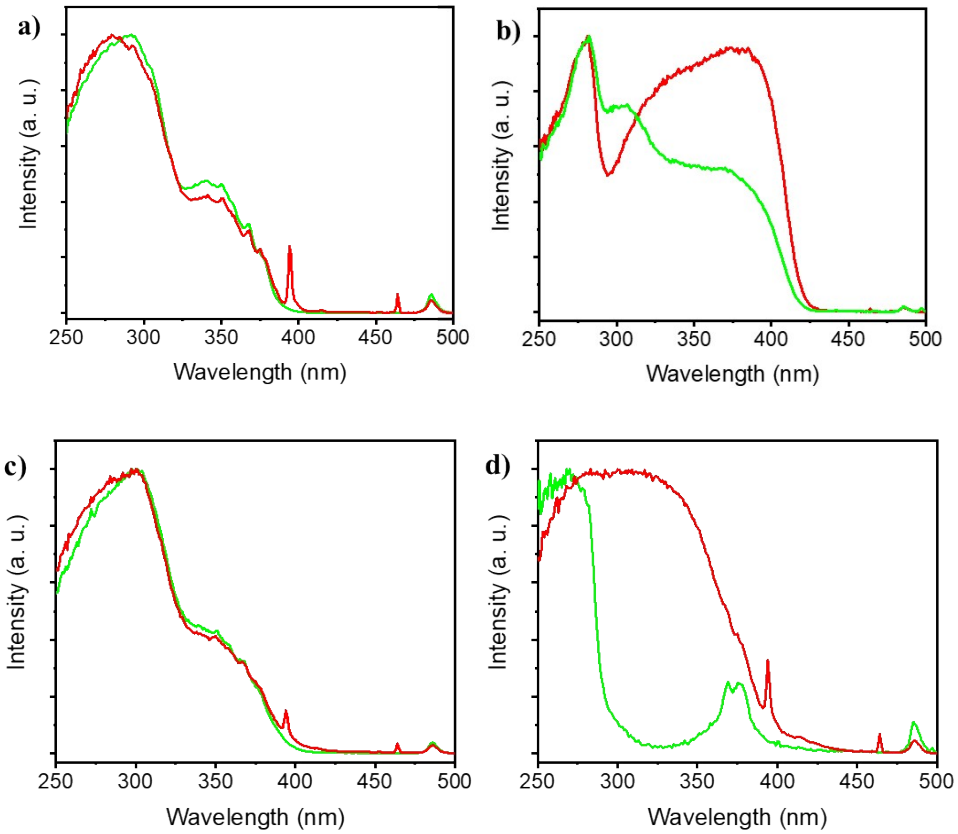

Figure S19: Room temperature excitation spectra of the exchanged MOFs a) **UCY-17**($Eu_{0.05}Tb_{0.95}$)/BDC, b) **UCY-17**($Eu_{0.05}Tb_{0.95}$)/ABDC, c) **UCY-17**($Eu_{0.05}Tb_{0.95}$)/FBDC, d) **UCY-17**($Eu_{0.05}Tb_{0.95}$)/NDC, monitoring the transitions $^5D_0 \nsim {}^7F_2$ of Eu^{3+} (red solid line, λ_{em} = 614 nm) and $^5D_4 \nsim {}^7F_5$ of Tb^{3+} (green solid line, λ_{em} = 543 nm) ions.

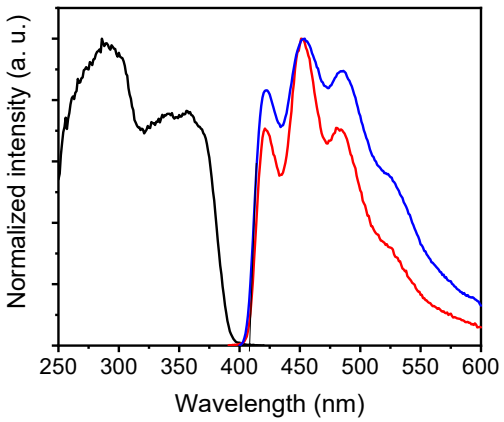

Figure S20: Normalized phosphorescence spectrum recorded at 77K of the pristine **UCY-17**(Gd) (blue solid line) (λ_{exc} = 301 nm, according to the excitation spectrum (black solid line)), and time-resolved phosphorescence spectrum at 77K integrated in a sweep range of 0.10 ms, to remove the fluorescence emission ($S_1 \nsim S_0$) (red solid line).

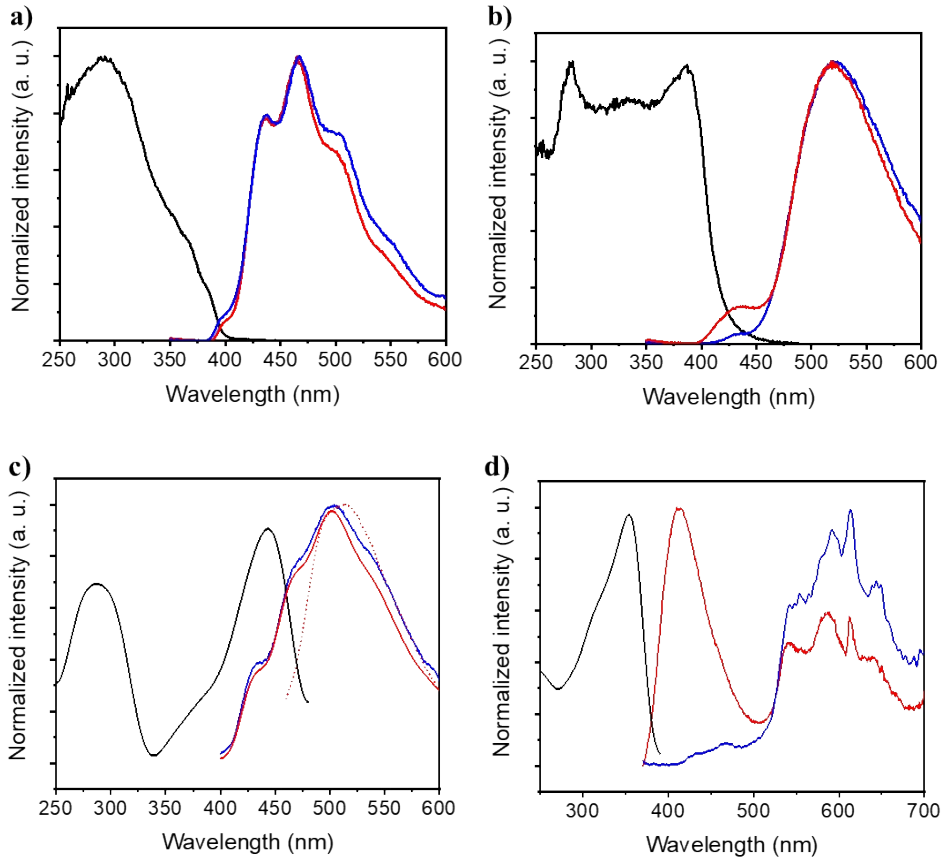

Figure S21: Normalized phosphorescence spectra recorded at 77K of the exchanged analogues **UCY-17**(Gd)/L (blue solid line) (excitation according to the excitation spectra (black solid line)), and time-resolved phosphorescence spectra at 77K integrated in a sweep range of 0.10 ms to remove the fluorescence emission (S_1 ✂ S_0) (red solid line) of a) **UCY-17**(Gd)/BDC, b) **UCY-17**(Gd)/ABDC, c) **UCY-17**(Gd)/FBDC (red dot line corresponds to the phosphorescence at λ_{exc} = 446 nm), d) **UCY-17**(Gd)/NDC.

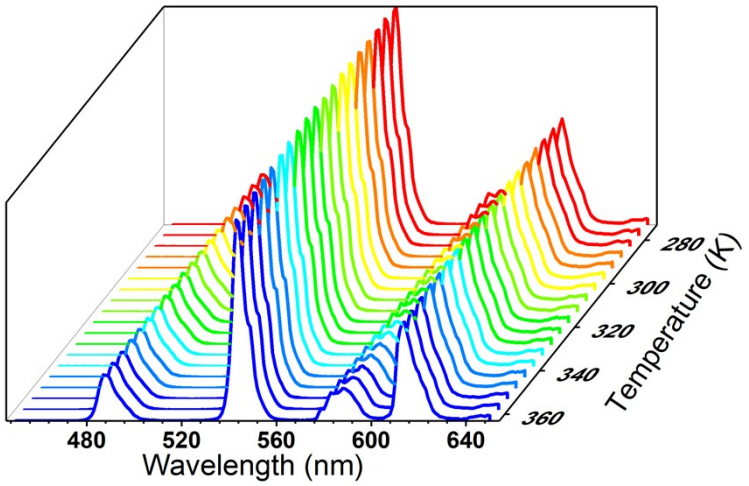

Figure S22: Thermal evolution of emission spectrum of the pristine MOF **UCY-17**($Eu_{0.05}Tb_{0.95}$) in the temperature range 270 - 360 K.

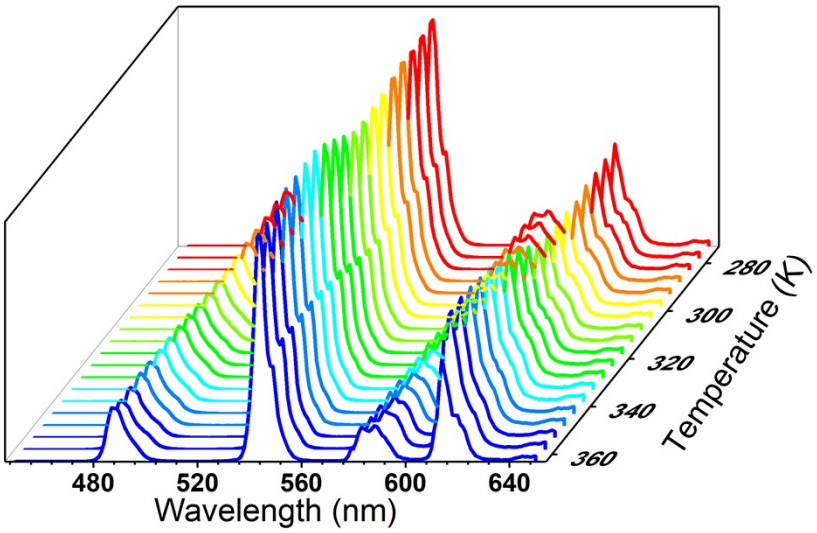

Figure S23: Thermal evolution of emission spectrum of compound **UCY-17**($Eu_{0.05}Tb_{0.95}$)/BDC in the temperature range 270 - 360 K.

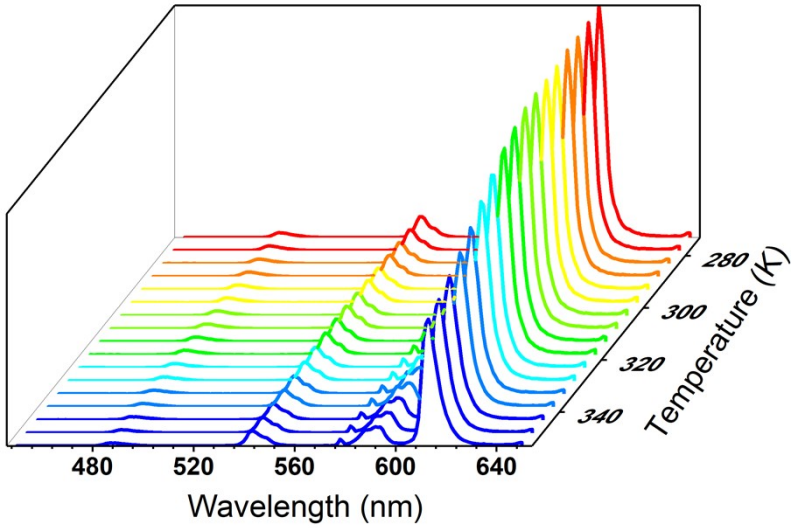

Figure S24: Thermal evolution of emission spectrum of compound **UCY-17**($Eu_{0.05}Tb_{0.95}$)/ABDC in the temperature range 270 - 360 K.

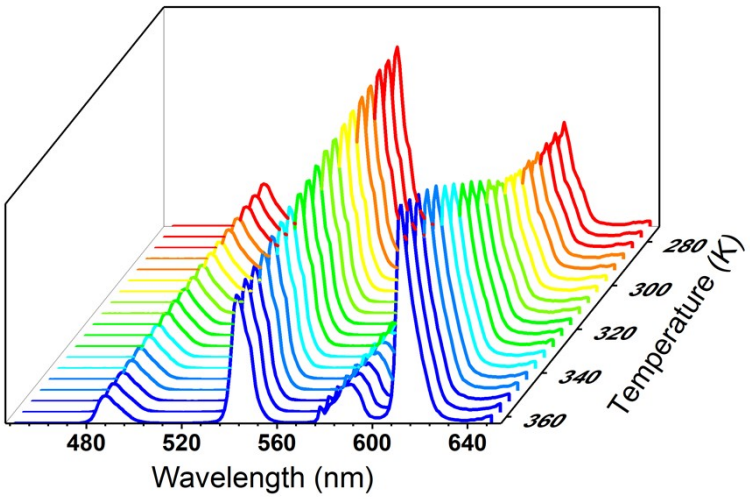

Figure S25: Thermal evolution of emission spectrum of compound **UCY-17**($Eu_{0.05}Tb_{0.95}$)/FBDC in the temperature range 270 - 360 K.

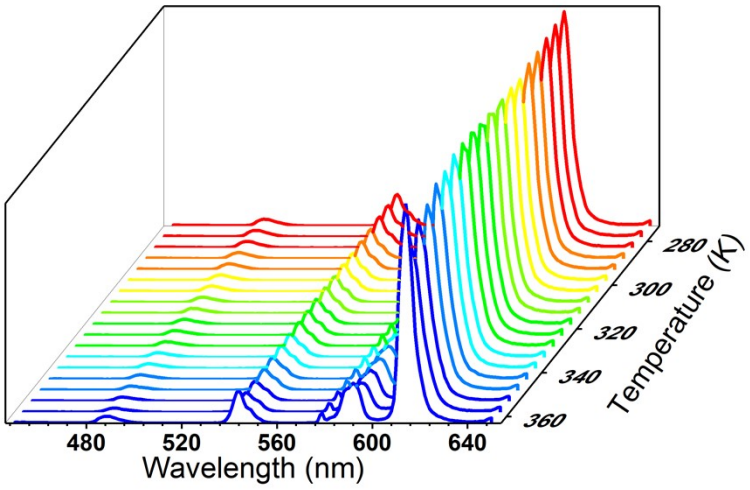

Figure S26: Thermal evolution of emission spectrum of compound **UCY-17**($Eu_{0.05}Tb_{0.95}$)/NDC in the temperature range 270 - 360 K.

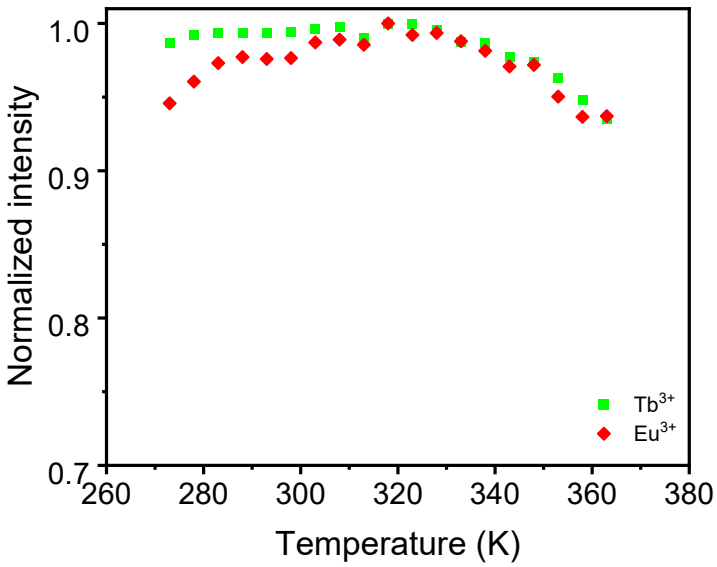

Figure S27: Thermal evolution of the integrated emission intensity of the pristine MOF **UCY-17**($Eu_{0.05}Tb_{0.95}$) in the temperature range 270 - 360 K.

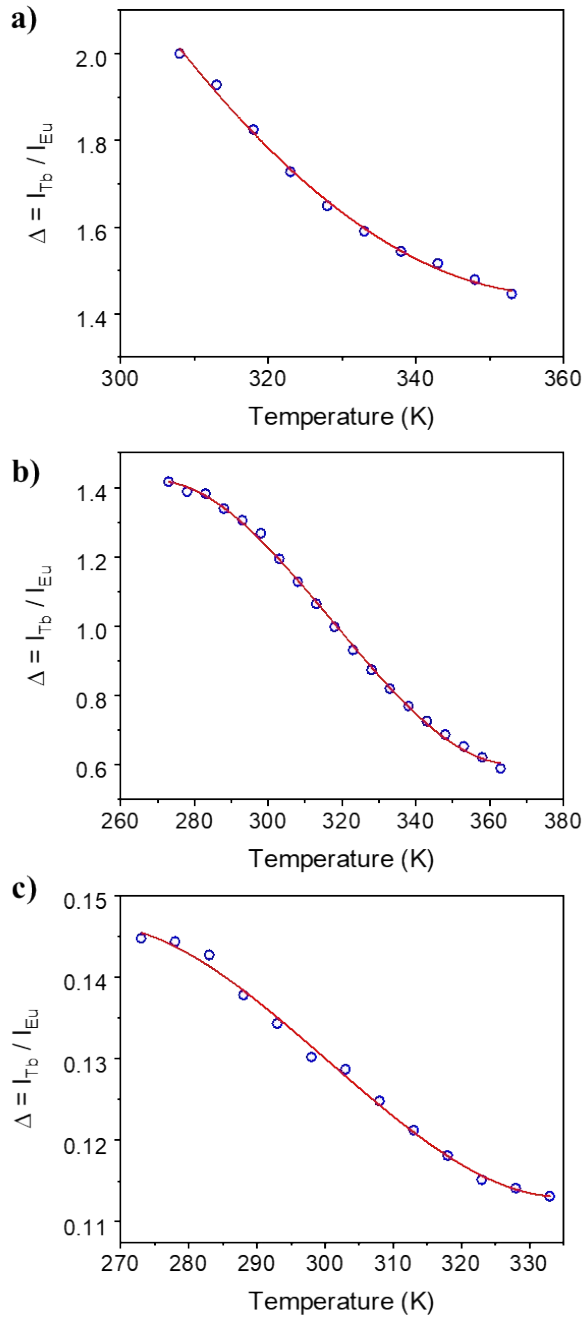

Figure S28: Temperature dependence of Δ in the indicated temperature range for the exchanged MOFs a) **UCY-17**($Eu_{0.05}Tb_{0.95}$)/BDC, b) **UCY-17**($Eu_{0.05}Tb_{0.95}$)/FBDC and c) **UCY-17**($Eu_{0.05}Tb_{0.95}$)/NDC. The red solid line represents the calibration curve obtained by the best fit of the experimental points to a polynomial equation ($r^2 > 0.990$). As the thermal quenching of Eu^{3+} and Tb^{3+} emission for **UCY-17**($Eu_{0.05}Tb_{0.95}$)/ABDC are nearly identical, the thermal evolution of the thermometric parameter for this exchanged analogue is not plotted.

Table S6. Chromaticity coordinates of the pristine **UCY-17**($Eu_{0.05}Tb_{0.95}$) and the exchanged analogues **UCY-17**($Eu_{0.05}Tb_{0.95}$)/L (L = BDC^{2-}, $ABDC^{2-}$, $FBDC^{2-}$ and NDC^{2-}) excited at various wavelengths (according to their respective excitation spectra).

Compound	(x;y) coordinates	λ_{exc} (nm)
UCY-17 ($Eu_{0.05}Tb_{0.95}$)	(0.4205; 0.5238)	301
UCY-17 ($Eu_{0.05}Tb_{0.95}$)/BDC	(0.4007; 0.5378)	278
UCY-17 ($Eu_{0.05}Tb_{0.95}$)/ABDC	(0.6134; 0.3740)	282
UCY-17 ($Eu_{0.05}Tb_{0.95}$)/FBDC	(0.4405; 0.5091)	301
UCY-17 ($Eu_{0.05}Tb_{0.95}$)/NDC	(0.6032; 0.3765)	280

Table S7. Fitting parameters of the polynomial equation ($Y = A + Bx + Cx^2 + Dx^3$) to the experimental curve $\Delta = f(T)$ for the exchanged analogues **UCY-17**($Eu_{0.05}Tb_{0.95}$)/L. Since the thermal quenching of Eu^{3+} and Tb^{3+} emission is nearly identical for **UCY-17**($Eu_{0.05}Tb_{0.95}$)/ABDC, it was more accurate to fit the thermal evolution of emission intensity data than these of the thermal evolution of the thermometric parameter.

Compound	Adjustment parameters	R^2
UCY-17($Eu_{0.05}Tb_{0.95}$)/BDC	$A = 28 \pm 2$ $B = -0.15 \pm 0.01$ $C = 2.1.10^{-4} \pm 0.2.10^{-4}$ $D = 0$	0.996
UCY-17($Eu_{0.05}Tb_{0.95}$)/ABDC	$I_{Tb} = f(T)$	
	$A = -245 \pm 54$ $B = 2.3 \pm 0.5$ $C = -0.007 \pm 0.001$ $D = 7.10^{-6} \pm 1.10^{-6}$	0.991
	$I_{Eu} = f(T)$	
	$A = -220 \pm 21$ $B = 2.0 \pm 0.2$ $C = -0.0061 \pm 0.0006$ $D = 6.1.10^{-6} \pm 0.6.10^{-6}$	0.999
UCY-17($Eu_{0.05}Tb_{0.95}$)/FBDC	$A = -54 \pm 5$ $B = 0.54 \pm 0.05$ $C = -0.017 \pm 0.0002$ $D = 1.8.10^{-6} \pm 0.2.10^{-6}$	0.999
UCY-17($Eu_{0.05}Tb_{0.95}$)/NDC	$A = -5 \pm 1$ $B = 0.05 \pm 0.01$ $C = -1.8.10^{-4} \pm 0.4.10^{-4}$ $D = 2.1.10^{-7} \pm 0.5.10^{-7}$	0.994

References

1. W. He, F. Du, Y. Wu, Y. Wang, X. Liu, H. Liu and X. Zhao, Quantitative ^{19}F NMR method validation and application to the quantitative analysis of a fluoro-polyphosphates mixture, *J. Fluor. Chem.*, 2006, **127**, 809.

2. N. Panagiotou, F. G. Moscoso, T. Lopes-Costa, J. M. Pedrosa and A. J. Tasiopoulos, 2-Dimensional rare earth metal-organic frameworks based on a hexanuclear secondary building unit as efficient detectors for vapours of nitroaromatics and volatile organic compounds, *Inorg. Chem. Front.*, 2022, **9**, 4850.